

# Influence of pulsed plasma treatment on phase composition and hardness of $\text{Cr}_3\text{C}_2$ -NiCr coatings

D.N. Kakimzhanov<sup>\*,1</sup>, B.K. Rakhadilov<sup>1,2</sup>, Yu.N. Tyurin<sup>3</sup>,  
O.V. Kolisnichenko<sup>3</sup>, L.G. Zhurerova<sup>1</sup>, M.K. Dautbekov<sup>2</sup>

<sup>1</sup>Sarsen Amanzholov East Kazakhstan university, Ust-Kamenogorsk, Kazakhstan

<sup>2</sup>Plasm.Science LLP, Ust-Kamenogorsk, Kazakhstan

<sup>3</sup>E.O. Paton Electric Welding Institute, Kiev, Ukraine

E-mail: dauir\_97@mail.ru

DOI: 10.32523/ejpfm.2021050106

Received: 01.03.2021 - after revision

In this study, the research results of the influence of pulsed plasma treatment on phase composition, hardness, and roughness of  $\text{Cr}_3\text{C}_2$ -NiCr coatings are presented. The  $\text{Cr}_3\text{C}_2$ -NiCr coating was applied to substrate 12Kh18N10T stainless steel by detonation spraying method. To change the physical and mechanical properties of sprayed coating's surface layers, subsequent pulse-plasma treatment was used. The pulse-plasma treatment leads to changing the roughness of  $\text{Cr}_3\text{C}_2$ -NiCr coating. The results of mechanical tests showed that after pulsed plasma treatment, the hardness of  $\text{Cr}_3\text{C}_2$ -NiCr coating is increased. Based on X-ray diffraction analysis, it was found that the hardness increasing of coating is associated with phase transformations on the surface layer, in particular, the formation of the oxide phase and an increase in the number of carbide particles.

**Keywords:** coating, detonation spraying, hardness, roughness, phase composition.

## Introduction

Currently, the application of protective coatings to improve the mechanical, physico-chemical and tribotechnical properties of metals and alloys, also products made from them are an actual area of materials science, solid state physics, plasma physics, chemistry, etc. [1-3].

$\text{Cr}_3\text{C}_2$ -NiCr coatings are widely used to protect against wear of working parts at high temperatures. The NiCr plastic metal matrix acted as a binder, supporting the brittle reinforcing phase of  $\text{Cr}_3\text{C}_2$  [4]. The application of such  $\text{Cr}_3\text{C}_2$ -NiCr coating can be produced using various gas thermal spraying methods, such as High Velocity Oxygen Fuel (HVOF) spraying, cold spraying, detonation spraying, atmospheric plasma spraying, etc. [5]. However, the presence of porosity and insufficient hardness of the coating can lead to premature failure of the structural elements working under conditions of intense wear. The sprayed coatings' physical and mechanical properties can be improved by subsequent treatment, such as laser beam-reflow, electron beam treatment, pulsed plasma treatment, etc. [6-10]. In this paper, we propose applying the pulsed-plasma method to treat  $\text{Cr}_3\text{C}_2$ -NiCr-based coatings to increase their hardness. Pulsed-plasma modification of the products' surface is carried out by the combined thermal and dynamic action of the plasma jet and the electromagnetic field. In this case, a shock-compressed layer of alloying elements from the ionic and atomic components of the plasma is formed on the product's surface. By changing the composition of the plasma, the composition of the surface layer can be controlled. Pulsed plasma surface treatment is a high-performance process of surface doping. The supply of the fuel mixture components to the pulsed plasma torch is carried out continuously, which simplifies (reduces the cost) the hardening technology and technological devices [11, 12].

In this paper cermet coatings ( $\text{Cr}_3\text{C}_2$ -NiCr) were studied. The coatings were manufactured by means of multi-chamber detonation spraying (MCDS). The influence of subsequent pulsed plasma treatment (PPT) of coatings on their phase composition and physical and mechanical properties is studied.

## Materials and research methods

The commercially available  $\text{Cr}_3\text{C}_2$ -25 wt% NiCr spray powder manufactured by H.C. Starck (584.054) was used as a feedstock material. The particle size distribution was in range –  $45+10\ \mu\text{m}$ . The coatings were applied to 12Kh18N10T substrate by detonation spraying on the MCDS installation [13]. In MCDS is realised mode of compressed detonation combustion of a gas mixture in specially profiled chambers. The accumulation of energy combustion from the two chambers in the cylindrical barrel provides the formation of a high-speed jet of combustion products, which accelerates and heats the sprayed powder. The detonation frequency rate was 20 Hz. The gases supply and powder was carried out continuously. Consumption of powder – 0.9 kg/h. The composition and consumption of components of the combustible gas mixture are shown in Table 1.

Table 1.  
Gas consumption.

Components of combustible mixture		Gas flow rate, m <sup>3</sup> /h
1 chamber	O <sub>2</sub>	2.92
	air	1.33
	C <sub>3</sub> H <sub>8</sub>	0.66
2 chamber	O <sub>2</sub>	2.93
	air	1.43
	C <sub>3</sub> H <sub>8</sub>	0.66
Gas transport (air)		0.9

Some of the coated samples were treated with pulsed plasma at the Impulse-6 set up. A feature of the used pulsed coaxial plasma generator is the possibility of commuting the electric current by the ionized gas region behind the detonation wave front [14]. This makes it possible to generate pulsed plasma with a frequency of 1-4 Hz and energy of up to 7 kJ. As a result, the surface experiences multiple pulsed thermal actions. The power density of the heat flow is  $10^4 \dots 10^6$  W/cm<sup>2</sup>. It is also possible to enter a complex of various doping elements into the plasma. PPT provides quick heating (heating time  $10^{-3} \dots 10^{-4}$  s) of the surface layer, followed by intensive cooling by removing heat into the product volume. The high rate (up to  $10^7$  K/s) of melting and crystallization of the surface layers contribute to the formation of a finely dispersed crystal structure and a high density of dislocations. Pulsed thermal action, elastic-plastic deformation of the structure of processed material, in combination with electromagnetic action due to the flow of pulsed current (up to 10 kA/cm<sup>2</sup>) through the treated surface layers, intensifies various physical and chemical processes. The pulse-plasma treatment parameters are given in Table 2.

Table 2.  
PPT parameters.

Parameter	value
Voltage on the plates of the capacitor bank (V)	3200
Capacity of the capacitor bank (μF)	960
Inductance of the discharge circuit (μH)	30
Pulse repetition frequency (Hz)	1.2
velocity of the plasma torch (mm/s)	5
distance from the sample (mm)	50

The phase composition was studied using traditional X-ray diffraction (XRD) methods, namely, the analysis of angular positions, intensities, and diffraction reflection profiles. The samples microhardness was measured in accordance with GOST 9450-76 (ASTM E384-11) on a Metolab 502 microhardness tester, with loads on the indenter P=1 N and a holding time of 10 s. Nanoindentation was performed on the nano-hardness tester NanoScan-4D Compact. In accordance with ASTM E384-11 Berkovich indenter 15 injections were conducted at a load of 100 mN. The Young's modulus and hardness were determined according to the method of Oliver and Pharr. The coatings surface roughness Ra was estimated using a profilometer model 130.

## Results and discussions

Obtained coatings thickness is about 200-230  $\mu\text{m}$ . Figure 1 shows surface micrographs and the measuring results of coatings roughness based on  $\text{Cr}_3\text{C}_2 + \text{NiCr}$ . Coatings surfaces have an inhomogeneous structure with pores. We chose parameter  $R_a$ , the arithmetic mean deviation of the profile, to be the main parameter characterizing coating roughness. The roughness parameter of the coatings obtained before plasma treatment has the values  $R_a = 11.2$ . And the coating, after 1 pass plasma treatment has  $R_a = 5.73$  roughness value and after 2 passes have  $R_a = 5.31$ , which is almost 2 times less than the roughness index before treatment. This is related the treatment of coating surface with a plasma jet, after which the particles or fragments of powder rising above the surface melt, and the surface roughness is reduced by  $\approx 48\%$ .

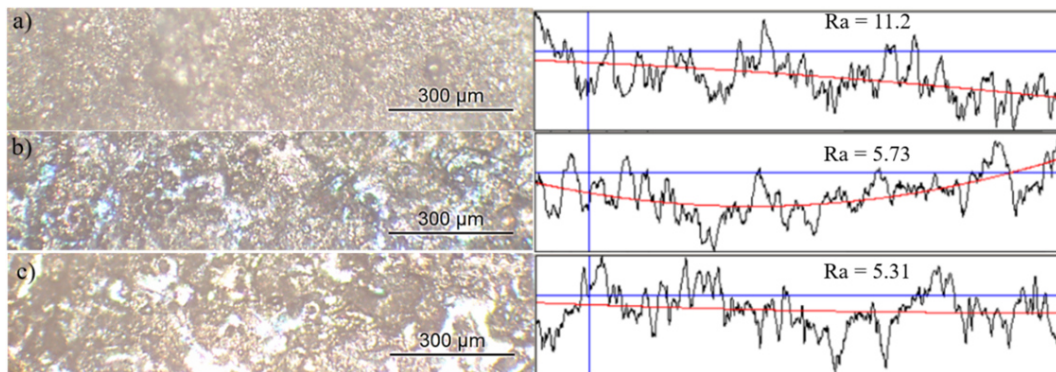


Figure 1. Micrographs and surface roughness of the  $\text{Cr}_3\text{C}_2$  coating: before plasma treatment (a), after 1 pass plasma treatment (b) and 2 pass plasma treatment (c).

Figure 2 shows results of X ray analysis of coating surface before and after pulsed plasma treatment. The following components of the phase components were detected in the coatings before treatment with a pulsed plasma jet: Ni-Cr-Fe,  $\text{Cr}_3\text{C}_2$ , Ni-Cr-Fe/ $\text{Cr}_7\text{C}_3$  and  $\text{Cr}_7\text{C}_3$  phases (Figure 2a). After treatment of the coating surface by the pulsed plasma method was revealed formation of the chromium oxide phase  $\text{Cr}_2\text{O}_3$  (Figure 2 (b, c)). With this, after 2 passes of the pulsed plasma jet on the diffractogram is observed increasing peaks intensity of  $\text{Cr}_3\text{C}_2$  chromium carbide, which indicates an increase in the content of  $\text{Cr}_3\text{C}_2$  carbide (Figure 2c).

Figure 3 shows a graph of the microhardness distribution over the coating thickness before and after pulsed plasma treatment. The graph of microhardness dependence on the depth of the  $\text{Cr}_3\text{C}_2$ -NiCr coating shows an uneven distribution of microhardness: the coating near the transition layer has a lower microhardness value, with differences to the near-surface layers. Coatings microhardness before pulsed plasma treatment was  $\approx 12$ , GPa (Figure 3a). Visible that after pulsed plasma treatment (Figure 3 (b, c)), the microhardness value increases and has a value after 1 pass of  $\approx 14.3$  GPa and after 2 passes of  $\approx 15.6$  GPa.

Figure 4 shows the dependences of the nanohardness (H, GPa) and the elastic modulus (Young's modulus E, GPa) on the coating depth. The nanohardness before the pulsed plasma treatment has values of 10.8 GPa (Figure 4a), and after the pulsed plasma treatment the coating nanohardness has values of 12.8

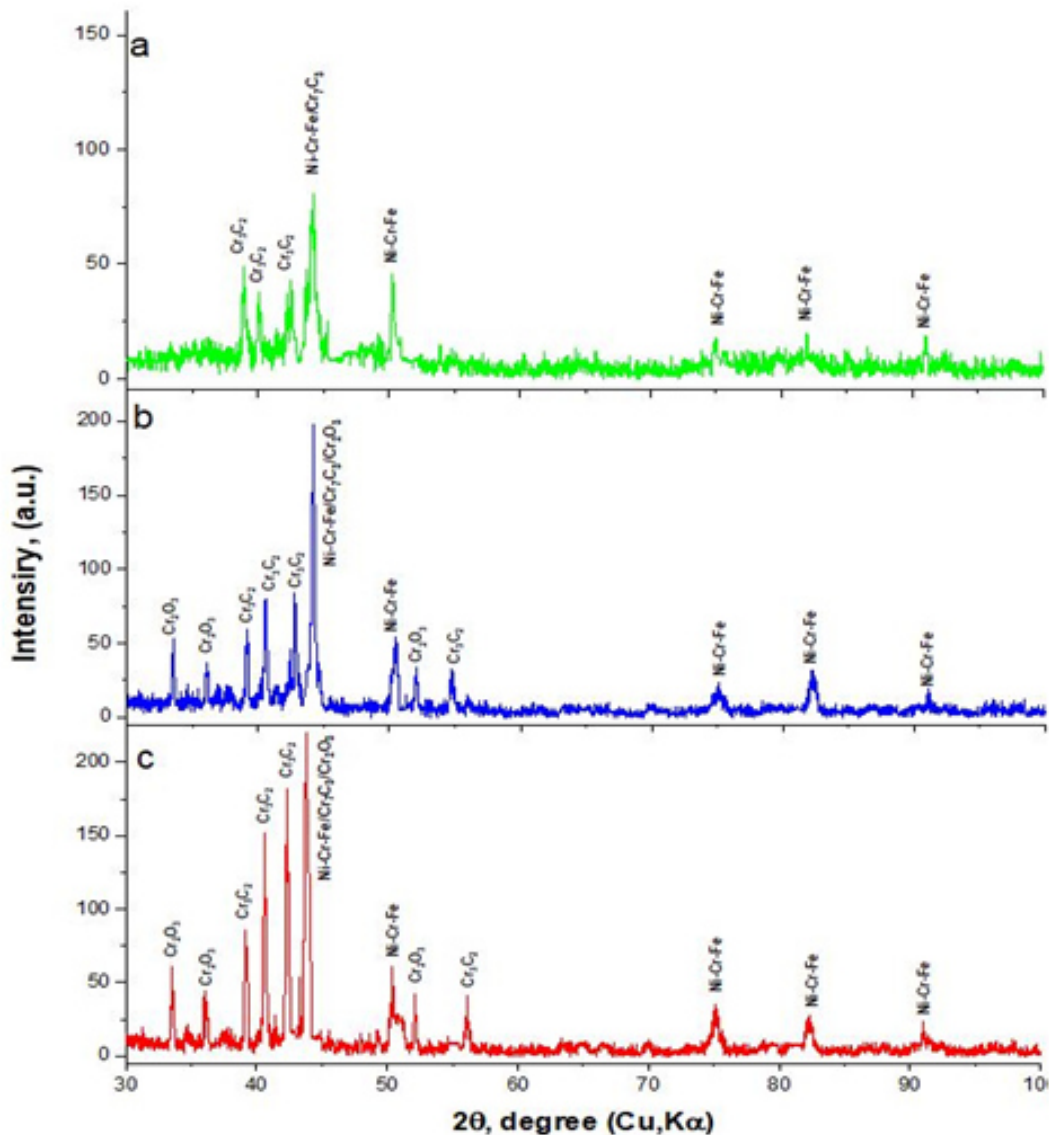


Figure 2. X-ray analysis results of  $\text{Cr}_3\text{C}_2$ -NiCr coating: before plasma treatment (a), after 1 pass plasma treatment (b) and 2 pass plasma treatment (c).

GPa (Figure 4b-1 pass) and 14.7 GPa (Figure 4c-2 pass), and coating elastic modulus before the pulsed plasma treatment is 240 GPa (Figure 4a), and after the pulsed plasma treatment with 1 and 2 passes respectively 261 GPa (Figure 4b) and 270 GPa (Figure 4c). The high hardness of the  $\text{Cr}_3\text{C}_2$ -NiCr coating after pulsed plasma treatment is explained by structural and phase transformations [15]. Based on X-ray diffraction analysis, it was found that the increase in the hardness of  $\text{Cr}_3\text{C}_2$ -NiCr coatings after pulsed plasma hardening is associated with increasing carbide particles in the near-surface layer, and it is associated with the formation of  $\text{Cr}_2\text{O}_3$  chromium oxide.

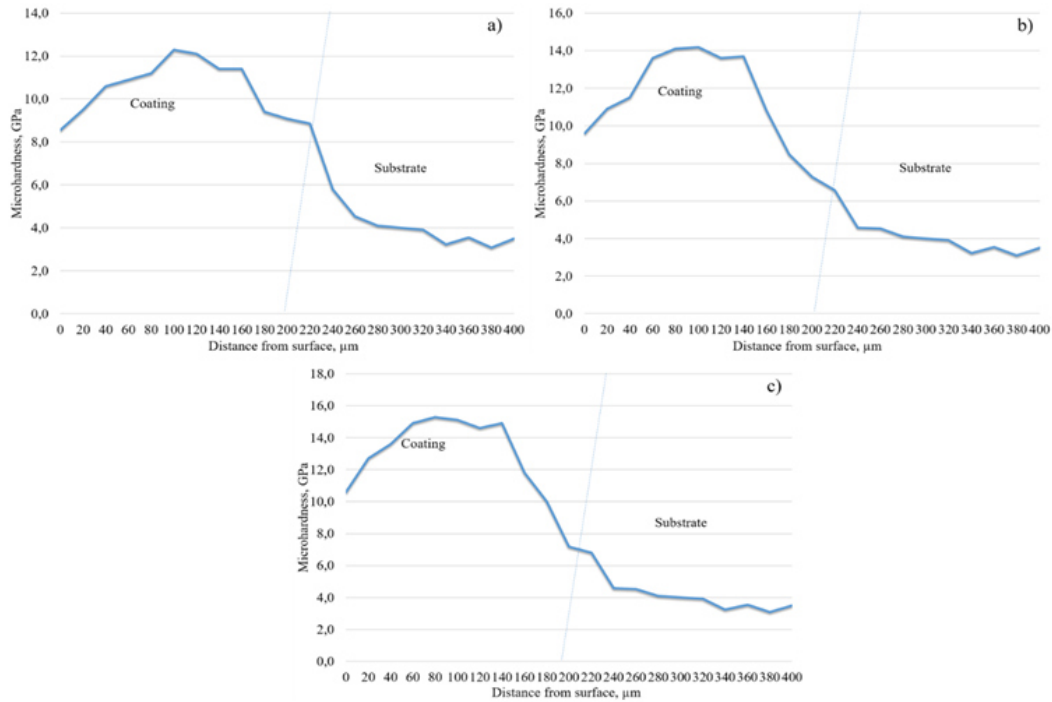


Figure 3. Graph of the hardness distribution over the depth of  $\text{Cr}_3\text{C}_2$ -NiCr coatings: before plasma treatment (a), after 1 pass plasma treatment (b) and 2 pass plasma treatment (c).

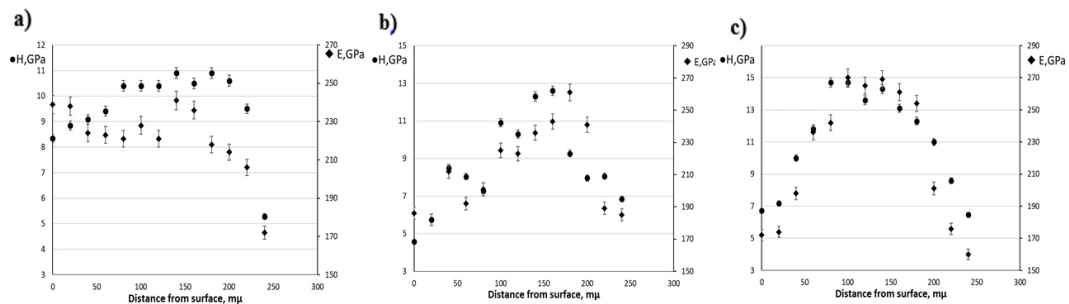


Figure 4. Distribution of hardness (H) and elastic modulus (E) over the depth of  $\text{Cr}_3\text{C}_2$ -NiCr coatings: before plasma treatment (a), after 1 pass plasma treatment (b) and 2 pass plasma treatment (c).

## Conclusion

Based on the obtained experimental data and their analysis, we reached the following conclusions: The pulsed plasma treatment leads to changing the surface morphology, in particular, after pulsed plasma treatment, the surface roughness reduced by  $\approx 48\%$ . After pulsed plasma treatment the microhardness of  $\text{Cr}_3\text{C}_2$ -NiCr coatings increases from  $\approx 12$ , GPa to  $\approx 15.6$  GPa. Based on X-ray diffraction analysis, it was found that the increase in the hardness of  $\text{Cr}_3\text{C}_2$ -NiCr coatings after pulsed plasma hardening is associated with increasing carbide particles in the near-surface layer, and it is associated with the formation of  $\text{Cr}_2\text{O}_3$  chromium oxide. As a result, the PPT can be recommended as a method for improving the complex physical and mechanical properties of pre-sprayed gas-thermal coatings.

## Acknowledgments

This paper was performed within the grant financing of scientific research of Committee of Science of the Ministry of Education and Science of the Republic of Kazakhstan. Grant AP09058615.

## References

- [1] A.D. Pogrebnyak et al., Structures and properties of hard and super hard nanocomposite coatings. *Ibid.* **52**(1) (2009) 29-54.
- [2] A. Cavaleiro et al., *Tekhnosphere* **1** (2011).
- [3] N.A. Azarenkov et al., Engineering of vacuum plasma coatings (2011).
- [4] A.D. Pogrebnyak et al., *Phys.-Usp.* **48**(5) (2005) 487-514.
- [5] M.K. Skakov et al., *Tsvetnye Metally* **1** (2017) 54-59.
- [6] B.K. Rakhadilov et al., News of the National Academy of Sciences of the Republic of Kazakhstan, Series of Geology and Technical Sciences **3**(441) (2020) 54-62.
- [7] J.R. Davis et al., *ASM Int.* (2004) 338.
- [8] D. Buitkenov et al., *Key Engineering Materials* **839** (2020) 137-143.
- [9] Ji-yu Du et al., *Surface and Coatings Technology* **369** (2019) 16-30.
- [10] J. Mateos et al., *Tribology International* **34**(5) (2001) 345-351.
- [11] Yu.N. Tyurin et al., *International Conference on Interaction of Radiation with Solids* **3** (1999) 214-217.
- [12] Yu.N. Tyurin et al., *Steel in Translation* **39**(10) (2009) 948-951.
- [13] O.V. Kolisnichenko et al., *Avtomaticheskaya-svarka* **10** (2017) 28-34. (in Russian)
- [14] Yu.N. Tyurin and O.V. Kolisnichenko, *The Open Surface Science Journal* **1** (2009) 13-19.
- [15] M.G. Kovaleva et al., *Journal of Nano-and Electronic Physics* **10**(6) (2018) 06035-1-06035-4.